

## Mössbauer spectroscopy of ion-bombarded material surfaces

S B OGALE, S V GHASAS, S M KANETKAR and V G BHIDE

Department of Physics, University of Poona, Pune 411 007, India.

**Abstract.** Recent trends in the field of ion bombardment of material surfaces are reviewed with a brief discussion about the present understanding of the subject. The use of novel characterization concepts to explore the ion beam-induced phenomena is emphasized and in this context the importance of the technique of conversion electron Mössbauer spectroscopy (CEMS) is brought out. A number of specific examples of the use of CEMS technique to studies on ion implantation, ion beam mixing and corrosion of ion-bombarded surfaces have been given.

**Keywords.** Mössbauer spectroscopy; ion bombardment; ion implantation; material surfaces.

### 1. Introduction

In recent years there has been an enormous growth of research activity in the field of materials science. The major attention of this activity is focussed on the question of obtaining material surfaces tailored to required specifications (Poate *et al* 1978, 1981; Gibbson *et al* 1981; White and Peercy 1980). The conventional techniques of equilibrium thermal treatment either for alloying, annealing or impurity diffusion cannot offer a useful solution to this problem because of various reasons which have been detailed elsewhere; the important one being the difficulty of adaptation due to non-availability of suitable process parameters. Hence during the past decade there has been considerable growth of interest in the use of radiation processing methods to obtain suitably tailored surfaces (Carter and Colligon 1968; Mayer *et al* 1970; Crowder 1973; Poate *et al* 1981; Hoonhaut 1981; Sood 1982). Amongst the radiation processing techniques generally employed, the prominent ones are ion implantation, ion beam mixing, laser treatment, electron beam treatment etc. In the present article we shall only discuss those techniques which are based on the use of energetic ion beams for processing of material surfaces.

The basic ion beam method of surface modification is ion implantation, in which selected ionic species having energy in the range of a few tens to a few hundreds of keV are bombarded on solids (Carter and Colligon 1968; Mayer *et al* 1970; Crowder 1973). This is a high vacuum ( $10^{-6}$  torr) process which offers a possibility of obtaining a specific dopant distribution in the submicron region below the solid surface by controlling the ion energy, target temperature, orientation of the target structure with reference to ion direction etc. Since the implantation energies used in most experiments are in the keV range, the atoms of solid which are displaced from their sites by the incoming ions also possess substantial energy to atomically displace other atoms on their track. Such sequential scattering events generate a zone in the neighbourhood of the track of the incoming ion, which is often referred to as a 'collision cascade region' (Poate *et al* 1981). The cascade formation occurs over a time scale of only  $10^{-13}$  to  $10^{-10}$  seconds rendering a highly non-equilibrium nature to the implantation process

and thus offering a possibility of synthesizing metastable surface alloys and solid solutions. This aspect is especially important in the context of metals, and metal-semiconductor systems, wherein one desires to obtain newer metastable solid solutions with novel application potentials. The process of direct implantation is however not suitable in applications which require high-concentration alloys because synthesis of such alloys requires bombardment at ion dose values as high as  $10^{17}$ – $10^{18}$  ions/cm<sup>2</sup>, and at such dose values the sputtering effect (Carter and Colligon 1968) erodes the presynthesized alloy layers. Thus it becomes necessary to find out alternative non-equilibrium methods of producing such metastable alloys in thin film form. It was shown by Tsaur *et al* (1979) that a simple but interesting variation of ion implantation method itself can be used to synthesize concentrated metastable alloys on the surface of any material without the intrinsic limitation imposed by the sputtering effect in the direct implantation case. This innovation is referred to as ion beam mixing.

The principle of ion beam mixing is depicted in figure 1. This technique is based on the fact that an energetic ion incident on a solid surface can dynamically move nearly hundred or more of the atoms of the surface layers over many lattice distances. Hence an ion dose of  $5 \times 10^{15}$  ions/cm<sup>2</sup> can lead to a dynamical mixing of  $10^{17}$  to  $10^{18}$  atoms in the surface layers of a solid. If these layers are composed of successively deposited thin films, an atomic mixing of these films can take place yielding a homogeneous high concentration alloy. Since the dose required to achieve alloying is almost two orders of magnitude lower in the case of ion beam mixing than that required in the direct implantation process, the sputtering limitation of the latter method is almost completely eliminated (Poate *et al* 1981). Also in view of the small dose, the percentage of the implanted ions in the composition of the mixed alloy is extremely small and thus beam mixing can be carried out by using any suitable ions of chemically inert gaseous species such as Ar<sup>+</sup>, Kr<sup>+</sup>, Xe<sup>+</sup> etc with little risk of influencing the physical properties of the alloy. It may further be observed that since the basic process used in ion beam

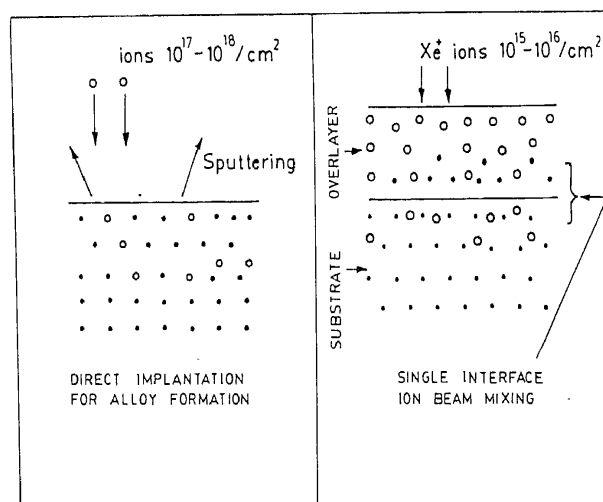


**Figure 1.** Schematic representation of ion beam mixing process when an energetic ion is incident on a thin film couple.

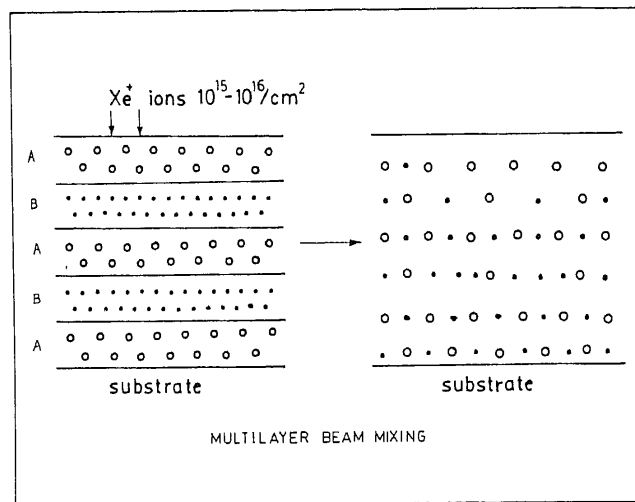


Figure 2. Ion beam mixing process in the case of a multilayered structure.

mixing is ion implantation itself, it preserves the most important advantage of the implantation method, *viz* its highly non-equilibrium nature which can lead to novel metastable structures and compositions. Also, the technique of ion beam mixing can be used effectively to tailor the composition of the mixed layer (figure 2). This can be achieved by preparing a layered structure of alloying elements having thicknesses suitable to yield specific final composition and subsequently mixing the deposited multilayered sandwich by energetic inert gas ions. In this multi-interface case, the energy of ions used to achieve mixing may be varied over a chosen range.

Considerable experimental work has already been done (Carter and Colligon 1968; Mayer *et al* 1970; Crowder 1973) in the area of ion bombardment of solids to understand the physical processes which can occur when radiation of a specific type is incident on the material surface. In most of these studies the techniques of Rutherford backscattering (RBS), x-ray diffraction (XRD), resistivity measurements etc have been employed and valuable information regarding the structural and chemical properties of processed layers has been obtained. Yet a need is felt for additional data, especially on the atomistic aspects of the beam-induced processes to understand the finer details of the nature and properties of the new materials which can be synthesized by the beam processing techniques. Amongst the characterization techniques which can directly address to the atomic level details, the technique of Mössbauer spectroscopy has a special place because, it can, in a single measurement, throw light on the structural, chemical, electrical and magnetic properties of materials as well as give valuable data on the defect complexes and their symmetries. Also this technique, being non-destructive in nature, does not forbid the use of other characterization concepts for studying the same material. Thus a coherent picture regarding the state of solid can be obtained without difficulty. Mössbauer spectroscopy provides a number of windows such as isomer shifts, quadrupole splitting, magnetic dipole interaction, Lamb-Mössbauer factor etc through which one can obtain extremely useful information about the nature of chemical environment, symmetry of the neighbours, magnetic field

at the nuclear site, dynamics of the Mössbauer atom etc (Bhide 1973). Yet, the use of this technique requires the presence of suitable isotopes of elements which can serve as source and absorber nuclei in a Mössbauer experiment, and as such this technique cannot be conveniently applied to the studies of arbitrarily chosen material systems. However, by appropriate choice of a representative Mössbauer system, the physics of the non-Mössbauer accessible materials can also be studied by this method.

The technique of Mössbauer spectroscopy can either be used in transmission mode or in scattering mode depending upon the need of the investigation. The scattering geometry, especially the one employing detection of conversion electrons emitted by the Mössbauer nuclei subsequent to gamma absorption, is particularly suited for studies of ion-irradiated surfaces because one can obtain Mössbauer information selectively from the submicron region below the solid surface which is primarily affected by the ion bombardment process (Sawicka and Sawicki 1981). In the case of iron ( $^{57}\text{Fe}$ ) the energy of conversion electrons is  $\sim 7.3$  keV and as such the electrons emitted within a depth of  $0.25 \mu\text{m}$  can only emerge out of the surface and be detected. The conversion electrons emitted from the sample surface are generally detected in a gas (He + 4% ethanol mixture) flow type of proportional counter in an integral manner and the Mössbauer information regarding the surface layers is obtained. Other detection schemes such as the ones employing channeltron type of detectors can also be employed but these are more sophisticated and expensive. In what follows we describe some results of conversion electron Mössbauer spectroscopic (CEMS) studies carried out on ion bombarded surfaces using simple gas flow type of proportional detectors.

## 2. Ion implantation: CEMS study

Sawicka and Sawicki (1981) studied the  $^{57}\text{Fe}$ -implanted Al, Si, Ge and diamond samples using CEMS technique. In the case of aluminium host, the effects of  $^{57}\text{Fe}$  implantation were studied (Sawicka *et al* 1978) over an ion dose range of  $10^{14}$  ions/cm<sup>2</sup> to  $2 \times 10^{17}$  ions/cm<sup>2</sup>. The maximum average ion concentration attained in aluminium is  $\sim 30\%$ , which is far above the solubility limit of iron in aluminium (0.001% at room temperature and 0.025% at 650°C). Some results of CEMS measurements on  $^{57}\text{Fe}$  implanted in aluminium are given in figure 3. The CEM spectra indicate a systematic variation of spectral features with change in the average iron concentration and this is irrespective of whether the concentration is achieved by variation of energy or dose. At iron concentrations smaller than 5% the spectra are composed of a singlet and a quadrupole split doublet. The single line can be attributed to iron monomers, while the doublet to higher iron associations (especially dimers) (Nasu *et al* 1980). As the average iron concentration is increased upto 5% the contribution of the single line decreases while that of the doublet increases systematically. The values of isomer shift corresponding to the two contributions show that the s-electron density at Fe-nucleus is larger in iron dimers than in monomers. In this case the CEMS technique also reveals that the iron aggregation process is enhanced both by implantation at high doses (leading to high defect concentrations) and by thermal treatment. In fact, the fast quenching nature of ion implantation process has a very significant contribution which can be seen from the fact that at dose values which are not high enough to lead to the formation of large iron clusters and yet high enough to surpass the limits of solid solubility, the contribution of iron monomers (non-associations) does appear in the CEM spectra. The Cracow group also studied  $^{57}\text{Fe}$  implantation effects in silicon

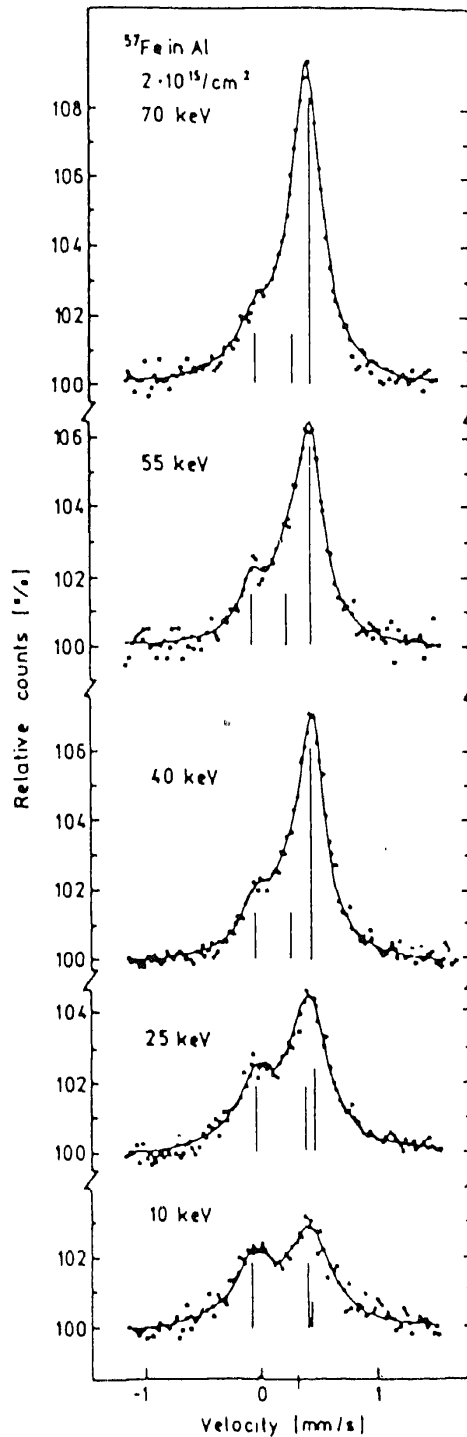


**Figure 3.** Variation of CEM spectra of <sup>57</sup>Fe implanted in Al with ion energy and therefore, with concentrations of implants ( $\bar{X} = 0.5\%, 0.6\%, 0.9\%, 1.1\%$  and  $2.1\%$  respectively). A single line is due to iron monomers and a doublet is due to iron dimers.

(Sawicka and Sawicki 1977) and germanium (Sawicki and Sawicka 1977) over a dose range between  $5 \times 10^{14}$  and  $5 \times 10^{16}$  ions/cm<sup>2</sup>. It has been shown that in Fe-Si, ion implantation leads to a broad doublet near the zero velocity channel indicating a distribution of hyperfine interaction which has a non-magnetic nature. The isomer shift and quadrupole splitting values corresponding to this doublet compare favourably with the parameters observed in the case of alloys formed by the coevaporation technique (Massenet and Daver 1976), thus establishing the rapid quenching nature of the implantation process. The appearance of this doublet can be attributed to the formation of iron dimers which occupy interstitial sites in the tetrahedral network and stabilize the amorphous surrounding, avoiding further clustering. The implantation studies on germanium (Sawicki and Sawicka 1977) also exhibit a number of interesting features regarding the relaxation in the implanted tetrahedral lattices, but the details of these studies will not be discussed here.

Dorik *et al* (1984) recently studied the oxidation properties of iron implanted with nitrogen ions by using the CEMS technique. In these experiments 80 keV N<sub>2</sub><sup>+</sup> ions were implanted on iron foils at a dose of  $2 \times 10^{16}$  ions/cm<sup>2</sup> and a number of such samples in the as-implanted form or subsequent to a vacuum annealing treatment were subjected to oxidation treatment in air at the temperature range of 300°C to 500°C for 4 min in each case. The CEMS as well as conventional gravimetric measurements performed on these samples revealed that the as-implanted samples exhibit an enhanced oxidation rate as compared to the virgin iron foils. If one compares the spectra of figures 4 and 5a which correspond to the unimplanted and implanted samples oxidized at 300°C for 4 min respectively, it is clear that the oxide components (Fe<sub>3</sub>O<sub>4</sub>) and (Fe<sub>2</sub>O<sub>3</sub>) are

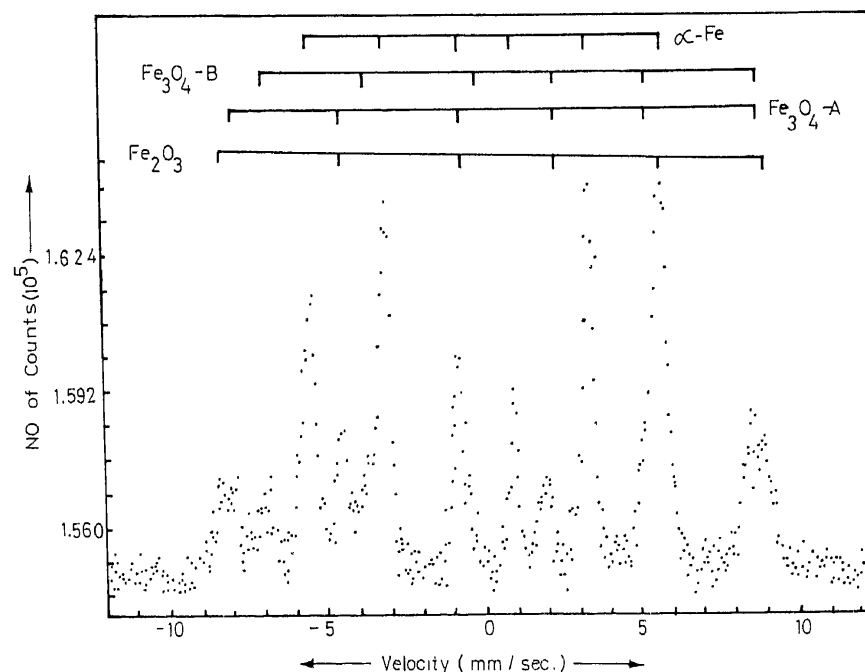
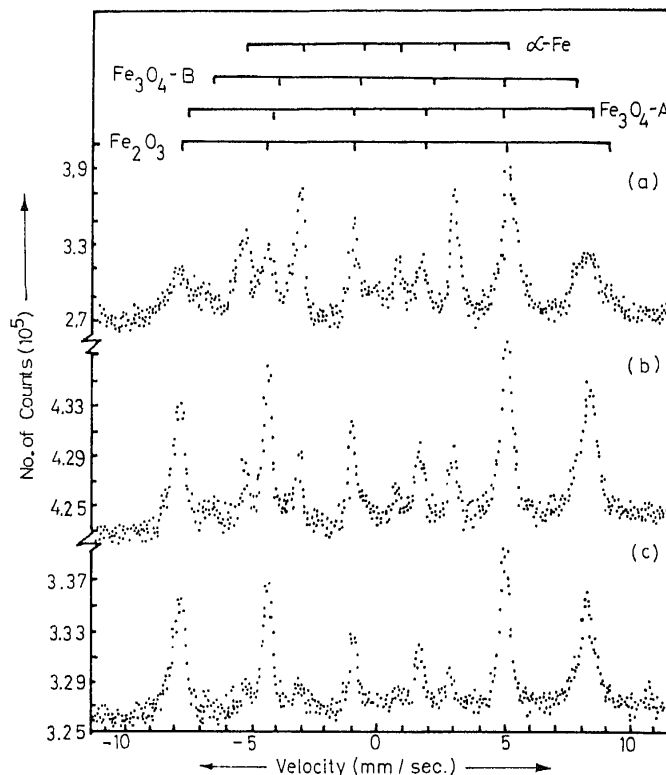
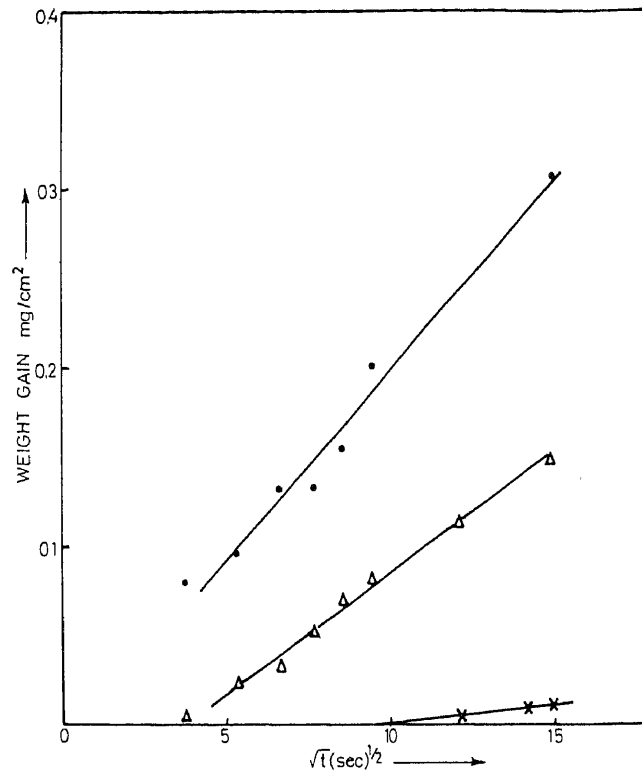


Figure 4. Room temperature CEM spectrum of iron foil heated at 300°C in air for 4 min.



**Figure 5.** Room temperature CEM spectra of  $N_2^+$  implanted iron foil heated in air at (a) 300°C, (b) 400°C (c) 500°C for 4 min each.

dominant in the implanted case when compared with the unimplanted sample. In fact, the ratio of the oxygen co-ordinated Fe to  $\alpha$ -Fe has a value of 3.6 in the implanted case as against 0.96 in the unimplanted sample. These differences in the oxidation rate are also reflected in the gravimetric measurements given in figure 6. When the implanted foil which is annealed in a vacuum of  $10^{-6}$  torr at 300°C for 30 min is oxidised, it shows a reduction in the oxidation rate even as compared to the rate exhibited by the virgin foil. This can be clearly seen by comparing the CEM spectra of figures 4 and 7a. The spectrum of figure 7a shows no detectable amount of oxide fractions indicating that the ion-implanted and vacuum-annealed foils show a significant improvement in the oxidation resistance of the virgin iron foils. This observation is confirmed by the gravimetric measurements given in figure 6. Figures 5 and 7 also show that at the oxidation temperature of 500°C both the implanted as well as the implanted and annealed foils exhibit considerable oxidation. It has been argued that ion implantation in iron produces defects and compressive stresses in the surface layers. Whereas the former effect enhances the oxidation rate due to defect-assisted diffusion, the latter effect tends to inhibit it, the overall effect in the implanted sample being a reduction in the oxidation resistance. The vacuum heat treatment (carried out at a temperature above the vacancy annealing temperature for  $\alpha$ -iron of 140°C but below its recovery temperature of 450°C) anneals out the point defects, stabilizes the compressive stresses and favours the



**Figure 6.** Results of gravimetric analysis for the unimplanted ( $\Delta$ ),  $N_2^+$  implanted ( $\cdot$ ),  $N_2^+$  implanted and annealed ( $\times$ ) iron foils heat treated in air at 300°C.

migration of the implanted nitrogen atoms towards the grain boundaries and dislocation pipes resulting in the short circuit paths for oxygen indiffusion getting blocked. This can lead to the observed oxidation inhibition.

The examples discussed above show that the CEMS technique has a tremendous potential in investigating the properties of ion-implanted metals and alloys containing a suitable Mössbauer accessible element such as Fe. Very recently it has also been demonstrated that the CEMS technique is equally powerful in studying the physics of ion beam-induced interface reactions, which have been a subject of considerable interest in recent years. In what follows, we briefly review some of this work.

### 3. Ion beam mixing: CEMS studies

The first experiments on the use of the CEMS technique to study ion beam-induced interface mixing and subsequent reactions were carried out very recently by the Poona University group (Godbole *et al* 1984a, b, 1985; Ogale *et al* 1985a, b; Patankar *et al* 1985). The ion beam-induced interface reactions in the single interface Fe-Al (Godbole *et al* 1984a, 1985; Ogale *et al* 1985), Fe-Si (Ogale *et al* 1985a) and Fe-Ge (Patankar *et al* 1985) structures have been investigated by this group using the  $^{57}\text{Fe}$  conversion



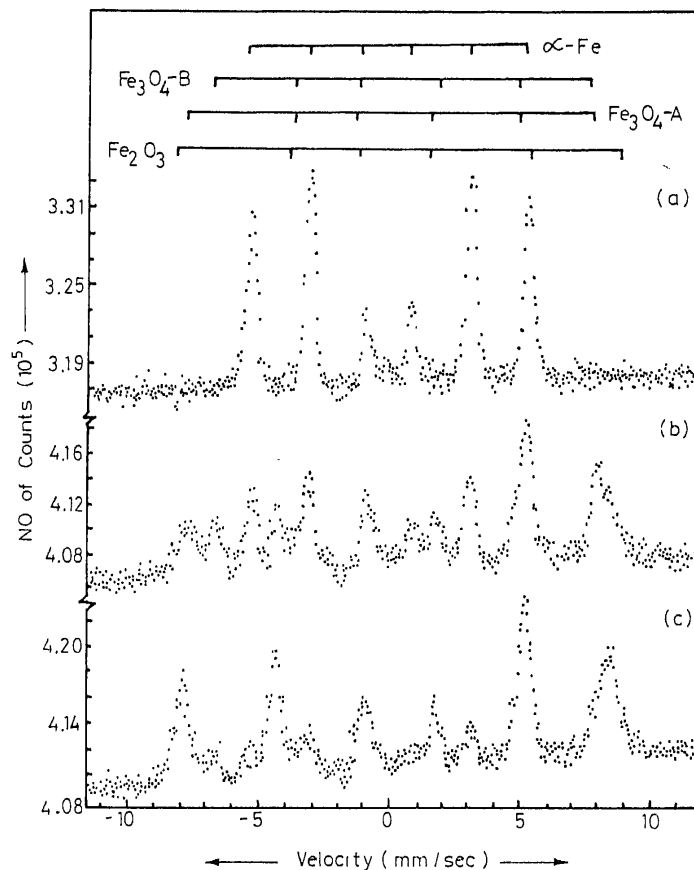


Figure 7. Room temperature CEM spectra of  $N_2^+$  implanted and vacuum annealed ( $300^\circ\text{C}$  for 30 min) iron foils heated in air at (a)  $300^\circ\text{C}$ , (b)  $400^\circ\text{C}$ , (c)  $500^\circ\text{C}$  for 4 min each.

electron Mössbauer spectroscopy; and interesting new information regarding the bombardment-induced interface phenomena has been brought out. In all these studies, an iron film (thickness  $\sim 300 \text{ \AA}$ ) was deposited onto the aluminium, silicon and germanium substrates conditioned by appropriate thermal and chemical treatments. Since ion beam mixing occurs at the interface and grows across it, a novel method of sample preparation was adopted to obtain the Mössbauer information predominantly from the interface region. For this purpose an  $\sim 50 \text{ \AA}$  film of  $^{57}\text{Fe}$  Mössbauer isotope enriched to 95.45% was deposited on the substrates of Al, Si and Ge, followed by a deposition of an  $\sim 250 \text{ \AA}$  thick film of natural iron which contains only 2.2% of the  $^{57}\text{Fe}$  isotope (figure 8). Since the Mössbauer signal emanates only from the  $^{57}\text{Fe}$  nuclei, by using this sample preparation procedure an interface sensitive CEM spectroscopic study could be carried out and the early interface reactions in the ion beam mixed region could be really understood.

The first system in which the ion beam mixing process was characterised by the interface sensitive CEMS technique was Fe-Al. This system was chosen for the following reasons (Godbole *et al* 1985): (i)  $^{57}\text{Fe}$ , a celebrated Mössbauer isotope is a constituent

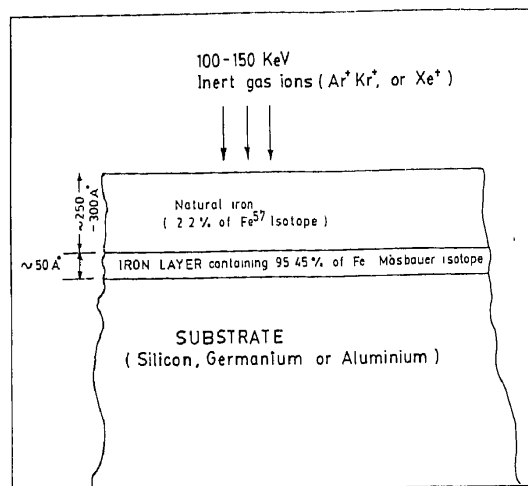
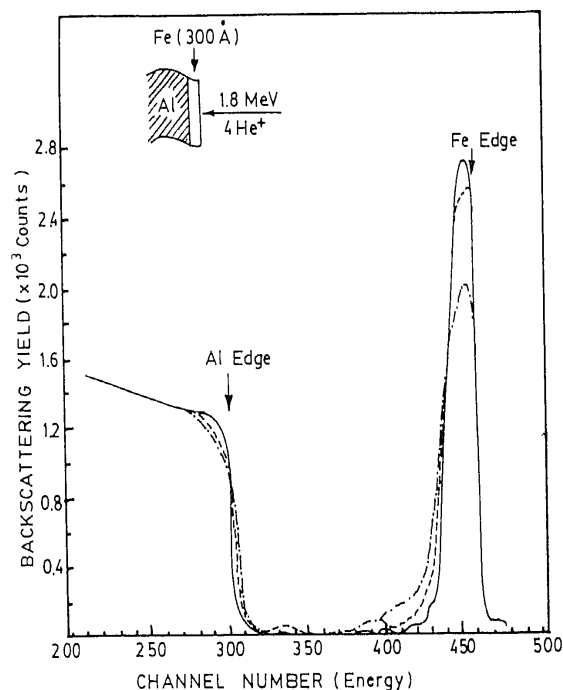


Figure 8. Sample for interface sensitive CEM spectroscopic studies.

of one of the components of this system; (ii) the equilibrium solid solubility of Fe in Al is extremely low *i.e.* only  $\sim 0.005$  at. % even upto  $450^\circ\text{C}$ , with the result that the conventional thermal treatment does not lead to any substantial interface reaction in this system; which enables one to clearly identify the characteristic differences between the ion beam induced and pure thermal reactions at the interface of two elemental solids; (iii) the phase diagram of the Fe-Al system is extensively investigated and it shows the existence of a large number of phases such as  $\text{Fe}_4\text{Al}_{13}$ ,  $\text{FeAl}$ ,  $\text{Fe}_2\text{Al}_5$ ,  $\text{Fe}_3\text{Al}$ ,  $\text{FeAl}_6$  etc., which is a favourable situation in so far as the occurrence of mixing at the interface is concerned, according to the empirical rule established earlier; (iv) Al being a low  $-Z$  material, it does not produce a high photoelectron background and thus the CEM spectra are expected to be of good quality in this system; and (v) Al being non-magnetic, it does not create any complications in elucidating the magnetic hyperfine interactions at the  $^{57}\text{Fe}$  nuclei. Many Fe-Al samples, prepared following the procedure mentioned above, were implanted with 100 keV  $\text{Ar}^+$  ions at a dose range between  $1 \times 10^{16}$  and  $3 \times 10^{16}$  ions/cm<sup>2</sup> to achieve the interface mixing. The fact that the interface mixing has occurred was confirmed by Rutherford backscattering measurements (figure 9), which also brought out the average composition of the mixed zone to be  $\text{Fe}_{5.5}\text{Al}_{4.5}$ . The as-deposited as well as ion beam mixed samples were annealed at a background vacuum of  $10^{-6}$  torr at various temperatures upto a maximum of  $600^\circ\text{C}$  and the transformations in the CEM spectra were monitored. All the spectra were computer-analysed following the conventional Mössbauer fitting procedure along with that for obtaining the distribution of magnetic hyperfine field (Window 1971).

The CEM spectra of the as-deposited sample and the corresponding hyperfine field distribution are shown in figures 10a and 10e respectively. In addition to the h.f. field of 330 kOe corresponding to  $\alpha$ -Fe, the h.f. distribution also shows another dominant magnetic interaction corresponding to a field value of 240 kOe, and an intense low field component which could indeed be due to the quadrupole and not the magnetic interaction. The h.f. field of 240 kOe corresponds to the presence of three aluminium neighbours at the sites of a number of  $^{57}\text{Fe}$  nuclei near the interface region. This can



**Figure 9.** Rutherford backscattering spectra (RBS) of the as-deposited and ion beam mixed composites. The continuous line corresponds to the as-deposited sample, the dashed line corresponds to the sample bombarded with 100 keV  $\text{Ar}^+$  ions at a dose of  $1 \times 10^{16}$  ions/cm<sup>2</sup> and the dash-dot line corresponds to the sample bombarded with 100 keV  $\text{Ar}^+$  ions at a dose of  $3 \times 10^{16}$  ions/cm<sup>2</sup>.

happen due to the deposition-induced reaction. The apparent low field magnetic component could indeed be fitted with a quadrupole doublet contribution having the h.f. interaction parameters of isomer shift  $\delta = 0.33$  mm/sec and the quadrupole splitting  $\Delta = 1.018$  mm/sec. The appearance of this doublet was attributed to the presence of  $^{57}\text{Fe}$  atoms in the  $\gamma\text{-Al}_2\text{O}_3$  skin on the surface of aluminium (Preston 1972) (this natural oxide of Al is always present on the aluminium surface in the form of an ultrathin film). When bombarded with  $\text{Ar}^+$  ions the CEM spectrum shows a drastic change [see figure 10b, f for the field distribution ( $P(H)$  curve)]. Figure 10f shows a considerable reduction of the peak at 330 kOe corresponding to  $\alpha\text{-Fe}$  and emergence of low field components at field values of 100 kOe, 192 kOe and 252 kOe. It may be hypothesized that the local atomic coordination in the ion beam mixed region fluctuates randomly between the aluminium-like (*i.e.* f.c.c.) and iron-like (*i.e.* b.c.c.) environments. It is possible to find a certain specific number of aluminium near-neighbours in the b.c.c. like (8 neighbours, Fe-b.c.c.) and f.c.c. like (12 neighbours, Al-f.c.c.) atomic environment by using the binomial distribution. From such a distribution one can deduce the distribution of internal field by assuming a lowering of the value of this field at  $^{57}\text{Fe}$  nucleus per aluminium neighbour to be  $\sim 26$  kOe (Oswald *et al* 1978). By this method one may expect to obtain a distribution which resembles at least certain portions of the observed  $P(H)$  distribution curve. This is indeed found to be true as seen

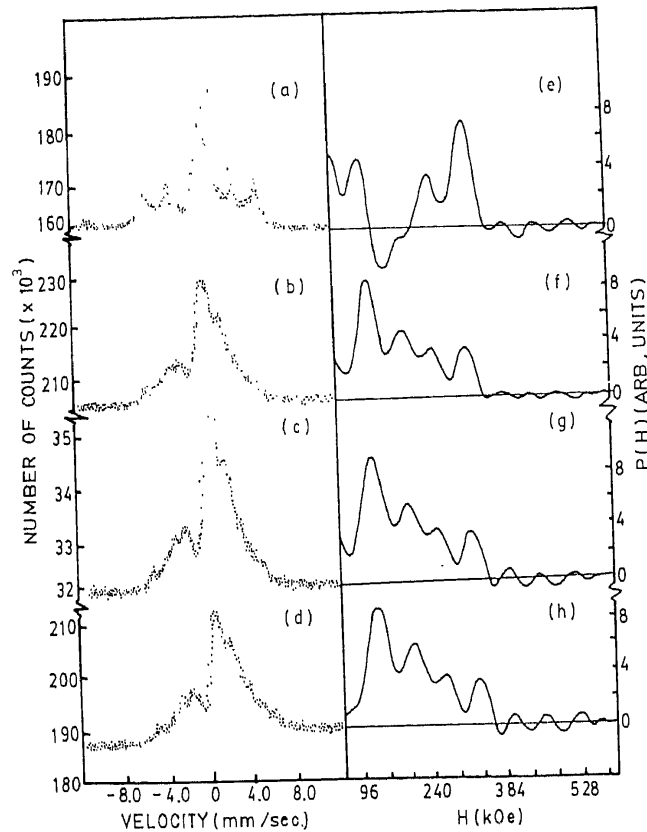


**Figure 10.** Room temperature CEM spectra of (a) as-deposited and (b) ion beam mixed Fe-Al composite. The spectra (c) and (d) represent ion beam mixed samples annealed at 300°C and 400°C respectively for 20 min each. The curves in (e), (f), (g) and (h) are the hyperfine field distribution plots corresponding to the spectra in (a), (b), (c) and (d) respectively.

from figure 11. The peaks at 192 and 252 kOe can thus be attributed to the fluctuations of atomic coordination between 8 and 12 neighbour environments. The peak at 100 kOe (lower field) can possibly be attributed to the dilute magnetic alloy of Fe in aluminium on the aluminium side of the interface.

When the ion beam mixed sample is annealed at 300°C and 400°C for 20 min in each case, the corresponding CEM spectra (figures 10c,d and the field distributions, figures 10g, h) do not show any significant changes from the characteristics exhibited by the ion beam mixed sample. When annealed at 500°C for 20 min, however, the spectral features show a drastic change, and the standard computer fitting procedure reveals the presence of  $\alpha$ -Fe and  $\text{Fe}_3\text{Al}$  phases (Gonser and Ron 1980) (figure 11) in the sample. This sample when further annealed at 600°C shows another drastic change in the CEM spectrum, which now indicates the presence of a small contribution of  $\alpha$ -Fe and a large contribution of a central doublet component. The h.f. interaction parameters corresponding to the doublet match reasonably well with the parameters corresponding to the iron clusters in aluminium matrix (Hirvonen and Raisanen 1982).

When the as-deposited sample was annealed at various temperatures upto 500°C, the

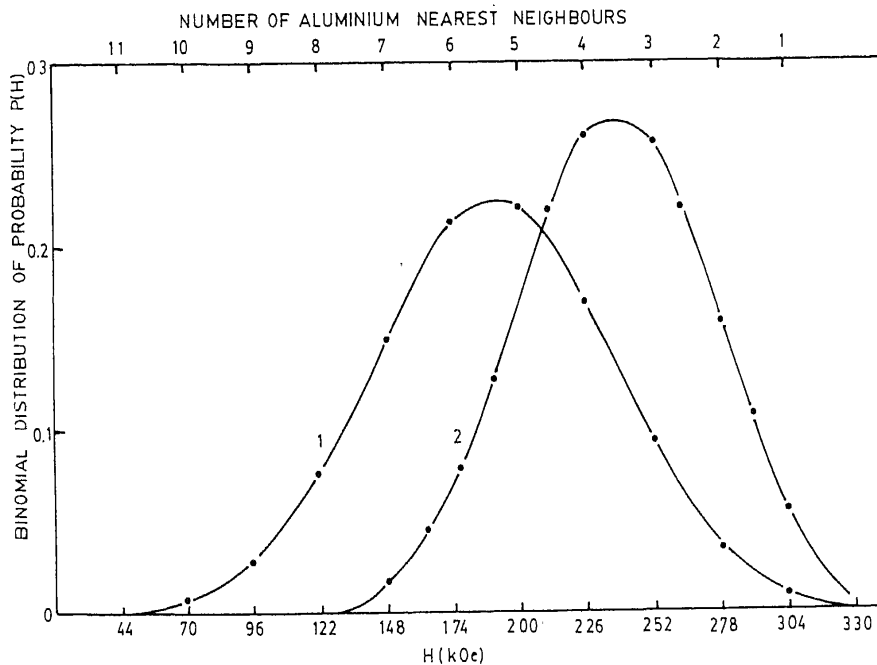
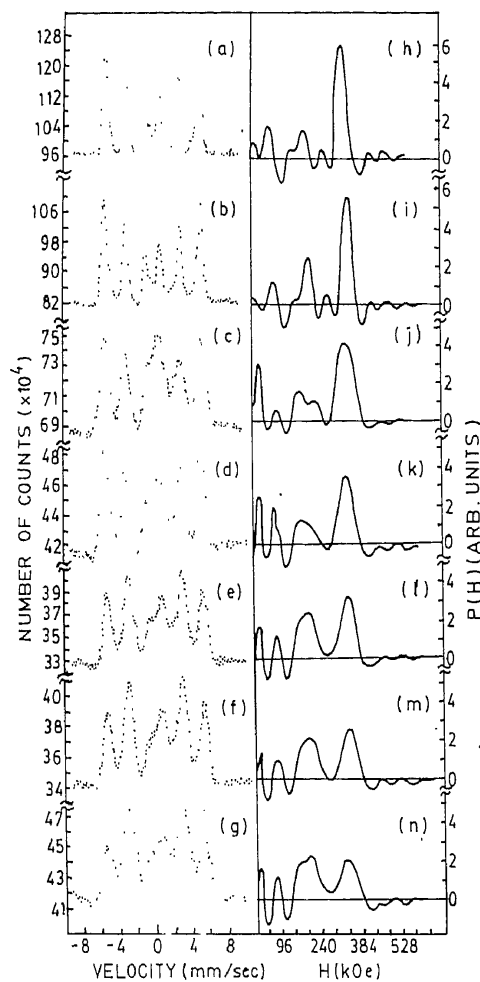


Figure 11. Probability distribution function  $P(n)$  for  $n$  Al to be near neighbours to Fe in a random alloy  $\text{Fe}_{55}\text{Al}_{45}$  using the standard binomial distribution and the corresponding hyperfine field distribution  $P(H)$  for local atomic coordination 12 (curve 1) and 8 (curve 2).

spectra continued to show the presence of  $\alpha$ -Fe with an increase in the intensity of this spectral component and a gradual reduction of the central doublet corresponding to  $^{57}\text{Fe}$  in  $\text{Al}_2\text{O}_3$  skin, which could be due to the out-diffusion of iron from the oxide. No  $\text{Fe}_3\text{Al}$  phase was observed in the as-deposited sample annealed at  $500^\circ\text{C}$ , which showed the presence of only  $\alpha$ -Fe. This clearly brings out the difference between the characteristics of the thermally-induced interface reactions in the as-deposited and ion beam mixed samples.

The Poona group has also studied the dose dependence of ion beam mixing at the Fe-Al interface (Ogale *et al* 1985b). For this purpose, non-interface sensitive studies were carried out in which the samples were prepared by depositing iron overlayer (containing  $\sim 30\%$  of the enriched  $^{57}\text{Fe}$  isotope uniformly distributed over the film region) onto the aluminium substrates. Such non-interface sensitive studies were undertaken primarily to understand the nature of the change in the beam mixing process when the ion dose is raised from a low value of less than  $\sim 5 \times 10^{14}$  ions/cm $^2$  at which individual cascade effects dominate, to the high doses at which the cascade overlap effects start playing an important role. The non-interface sensitive method was used in the place of the interface sensitive one in these studies because the interface sensitive technique defines a fixed length scale (of  $\sim 50$  Å) at the interface, which is not compatible to the growth of the mixed region as a function of the increase of the ion dose. The results of the non-interface sensitive CEMS studies are shown in figure 12. In figure 12a the CEM spectrum of the as-deposited sample is shown while in 12b to 12g the



**Figure 12.** Room temperature CEM spectra of (a) as deposited Fe-Al composite and ion beam mixed Fe-Al composite with a dose of (b)  $1 \times 10^{14}$  ions/cm<sup>2</sup> (c)  $5 \times 10^{14}$  ions/cm<sup>2</sup> (d)  $1 \times 10^{15}$  ions/cm<sup>2</sup>, (e)  $5 \times 10^{15}$  ions/cm<sup>2</sup>, (f)  $1 \times 10^{16}$  ions/cm<sup>2</sup>, (g)  $3 \times 10^{16}$  ions/cm<sup>2</sup>. The corresponding hyperfine field distribution curves are represented with continuous curves.

CEM spectra of the composites implanted with Ar<sup>+</sup> ions at various values of ion dose ranging between  $10^{14}$  ions/cm<sup>2</sup> and  $3 \times 10^{16}$  ions/cm<sup>2</sup> are shown. The distributions of internal magnetic field have also been given for all the spectra. The distribution corresponding to the as-deposited sample exhibits a peak at 330 kOe (which corresponds to  $\alpha$ -Fe) and other small variations which can partly be attributed to the use of Fourier series in the decomposition procedure upon ion beam mixing. With increasing implantation dose the peak at 330 kOe shows a systematic decrease in intensity with emergence of peaks corresponding to lower values of hyperfine fields. Also the line-widths of the Mössbauer spectral components show an increase with implantation dose, indicating the presence of disorder in the mixed zone. The emergence of peaks corresponding to lower field values is due to formation of an

interface alloy in which the  $^{57}\text{Fe}$  nuclei find one or more of aluminium neighbours which contribute to the decrease of hyperfine field. When integrated over the entire range of lower field values distinguishable from the peak at 330 kOe, the total low field contribution shows a gradual increase with ion dose (figure 13). It may be noted, however, that the increase is almost linear upto a dose of  $10^{15}$  ions/cm $^2$  beyond which the nature of the curve and hence possibly the mixing process, shows a deviation (Poate *et al* 1981). It is interesting to note that the dose value of  $10^{15}$  ions/cm $^2$  is typically the value at which the cascade overlap effects may be expected to dominate the mixing process. It is possible to separately fit the low field components of the Mössbauer spectra by the standard Mössbauer fitting procedures and to identify the nature of the microstructure. This exercise is presently being carried out.

In addition to the Fe-Al system, the Fe-Si (Ogale *et al* 1985a) and Fe-Ge (Patankar *et al* 1985) systems have also been investigated by the Poona group. The Fe-Si system exhibits features similar to those observed in the Fe-Al system, though at a relatively higher temperature. On the other hand, the Fe-Ge system exhibits a behaviour which is distinctly different as compared to the Fe-Al and Fe-Si systems. In the Fe-Ge case the transformations are more gradual and the Fe-enrichment process begins at a temperature as low as 350°C. The similarities and differences in the behaviour exhibited by the three systems correspond reasonably well to the atomic and solid state parameters of the elements involved.

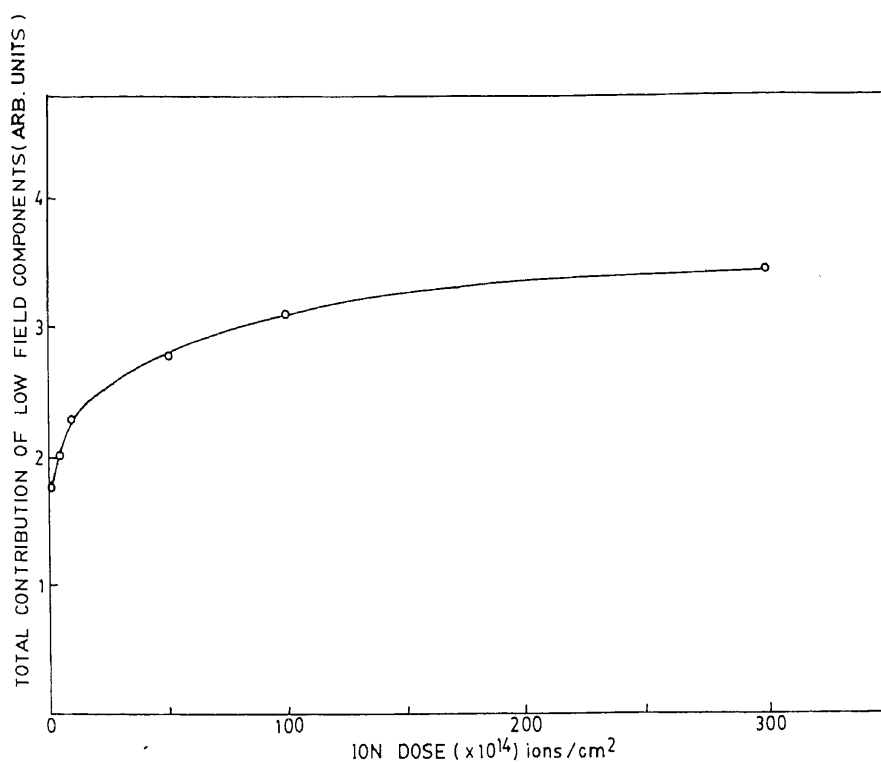
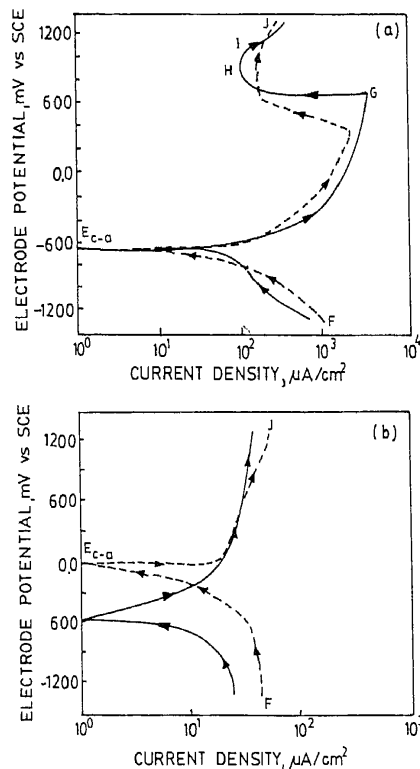


Figure 13. Total contribution of low field component as a function of ion dose for Fe-Al composite.

In the earlier paragraphs we have discussed the work of basic nature concerning the ion beam mixing process carried out by employing the CEMS technique. Using the same technique the Poona group has also investigated the applied nature on the ion beam mixed state of Fe-Al alloy, in which the electrochemical corrosive properties of this alloys have been studied (Kanetkar *et al* 1985). In these experiments the as-deposited as well as ion beam mixed Fe-Al samples prepared for interface sensitive CEMS measurements were subjected to electrochemical corrosion by employing the three sweep potentiokinetic polarization technique. The use of the three sweep technique, suggested by Ashworth *et al* (1976) for electrochemical studies of corrosive properties of implanted solids was made to eliminate any possible interference of the air-formed oxide film in the evaluation of the corrosive properties of the ion beam mixed region. We carried out potentiokinetic polarization measurements at two sweep rates. A sweep rate of 1.33 mV/sec corresponding to a quasi-steady state condition was used to simulate the situation of practical importance, while a higher sweep rate of 10 mV/sec was used to understand the dynamical features of the corrosive activity. A higher sweep rate is also useful to obtain a clear active-to-passive transition in cases where such a transition cannot be seen, in view of the thinness of the films as compared to the length scale of corrosive activity. The electrochemical corrosion was measured at room temperature in an acetic acid/sodium hydroxide buffer solution having a pH of 6.95.

From figure 14, it is observed that the Fe foil shows active-to-passive transition for



**Figure 14.** Second positive going sweep in the three sweep potentiokinetic polarisation curves for (a) pure iron foil (b) pure aluminium foil. The continuous line and dashed curves correspond to sweep rates of 1.33 mV/sec and 10 mV/sec respectively.



both the sweep rates. The values of critical current density and pitting potential are lower in the higher sweep rate as compared to the lower sweep rate. In aluminium, no active-to-passive transition is observed at either values of the sweep rate (figure 14b), because subsequent to an initial dissolution, the passivation ensues almost immediately due to the formation of an aluminium oxide coating in the aqueous medium.

When the as-deposited sample was subjected to electrochemical corrosion, the iron layers deposited on the aluminium substrates dissolved for both the sweep rates employed. On the other hand, the ion beam mixed Fe-Al sample exhibited distinctly different features as compared to as-deposited Fe-Al sample (figures 15 and 16). An examination of figures 15a, b clearly shows that the dissolution of iron is considerably higher in the as-deposited sample as compared to the ion beam mixed sample. This is indicated by the current density corresponding to the point D on the curve of the first negative going sweep. It is also observed that the as-deposited sample does not show any active-passive transition and indicates a dissolution similar to that of pure aluminium. At faster sweep rate (figure 16) the active-to-passive transition and the corrosion inhibition in ion beam mixed sample are seen more clearly.

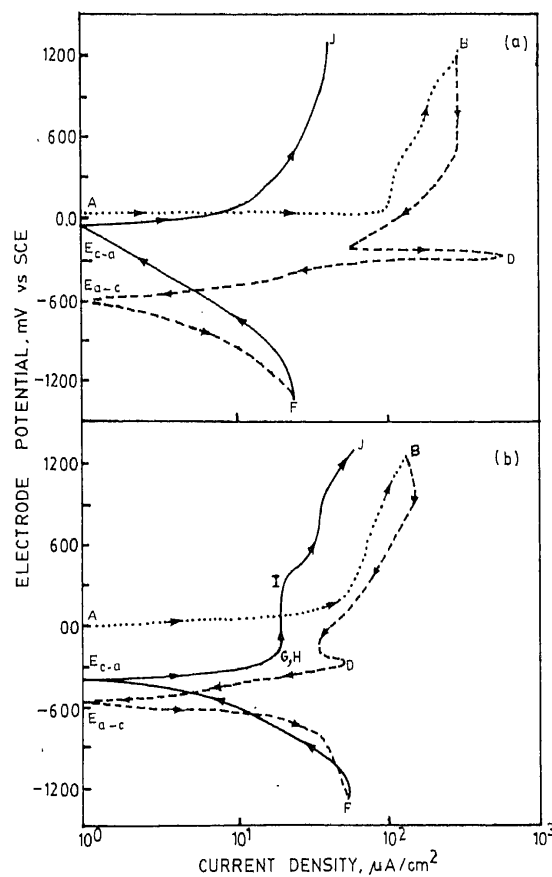


**Figure 15.** Three sweep potentiokinetic polarisation curves for (a) as-deposited and (b) ion beam mixed, Fe-Al composite. The dotted curve corresponds to first positive going sweep, the dashed curve corresponds to first negative going sweep and the full line curve corresponds to second positive going sweep at the sweep rate of 1.33 mV/sec.

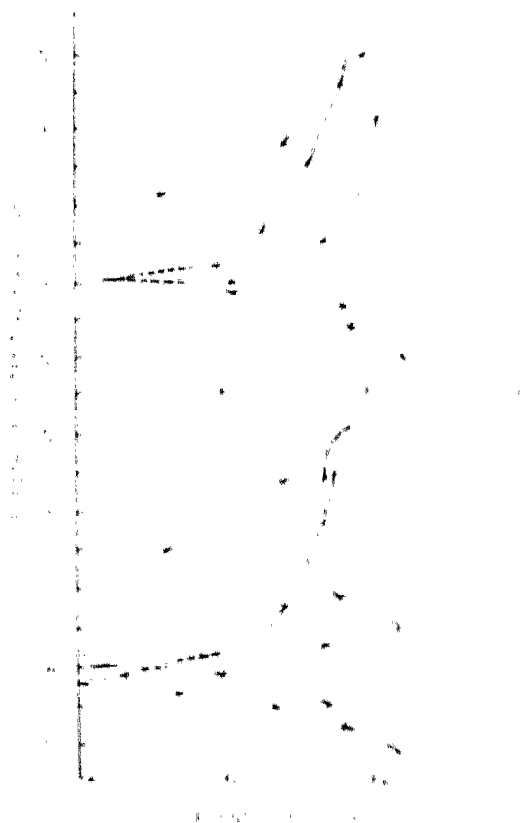
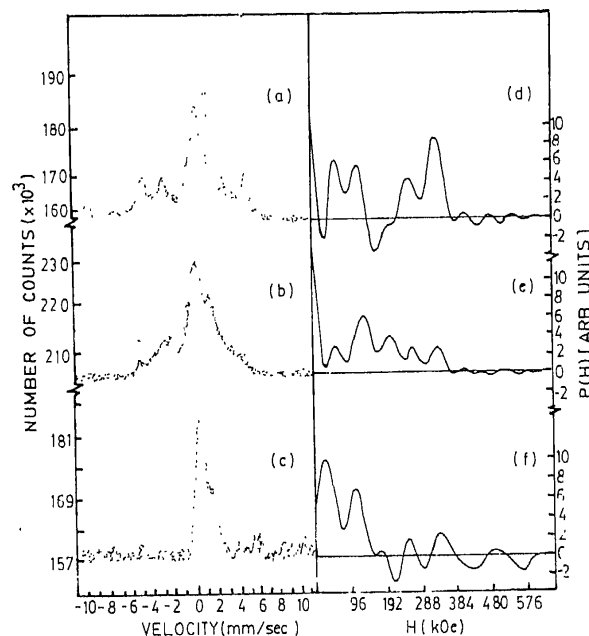


Figure 16. Three sweep potentiokinetic polarization curves for (a) as deposited and (b) non beam mixed Fe-Al composite. The dotted curve corresponds to first positive going sweep, dashed curve corresponds to the first negative going sweep and the solid curve corresponds to second positive going sweep at the sweep rate of  $10 \text{ mV/s}$ .

In order to understand the physics of the corrosive properties exhibited by the non-beam mixed sample we characterised this sample before and after the corrosive action by using the cFM technique. The cFM spectrum of the non beam mixed sample (figure 17b) is significantly different as compared to that of the deposited sample (figure 17a) and the corresponding magnetic field distribution (figure 17c) shows four peaks at 100, 192, 252 and 330 kOe. On comparing figure 17d) with figure 17c), it is clearly seen that the peak at 330 kOe which corresponds to  $\alpha$ -Fe is considerably reduced and low field components are increased upon ion bombardment. This means that significant atomic mixing has occurred at the interface. The average composition of the mixed layers obtained by RBS technique turns out to be  $\text{Fe}_{55}\text{Al}_{45}$ . The details of this cFM spectrum and the corresponding field distribution have already been discussed earlier in this paper. In the present context it may only be mentioned that the ion beam mixed interface is a disordered alloy with significant fluctuations in local alloy structure and composition.

As mentioned earlier, the as-deposited Fe-Al sample shows complete dissolution of iron overlayer when subjected to electrochemical corrosion. To confirm the complete



**Figure 17.** Room temperature CEM spectra of Fe-Al composite: (a) as-deposited (b) ion beam mixed and (c) ion beam mixed composite subjected to aqueous corrosion. Hyperfine field distributions corresponding to the spectra in (a), (b) and (c) are shown in (d), (e) and (f) respectively.

absence of Fe, we recorded the CEM spectrum of the as-deposited sample after electrochemical corrosion. No resonant absorption could be seen showing a complete dissolution of the iron film. On the other hand, the ion beam mixed sample led to CEM spectrum as shown in figure 17c. When decomposed, this spectrum gives magnetic hyperfine field distribution as given in figure 17f. It can be readily seen that the peaks at 192 and 252 kOe in the field distribution corresponding to the ion beam mixed sample are decreased substantially upon corrosion while the peak at  $\sim 100$  kOe is shifted to a lower field value of  $\sim 90$  kOe. It is also observed that the peak at 330 kOe is decreased to a certain extent. In addition to these changes in the magnetic components we could fit the total spectrum of figure 17c with two quadrupole-split doublets. One of the doublets has an isomer shift of 0.40 mm/sec and a quadrupole splitting of 0.63 mm/sec, while the other doublet has an isomer shift of 0.89 mm/sec, and a quadrupole splitting of 1.27 mm/sec. The hyperfine parameters of the latter doublet match reasonably well with those of FeO (Terrell and Spijkerman 1968; O'Grady 1980; Eldridge *et al* 1982) (I. S. = 0.91 mm/sec, Q. S. = 0.80 mm/sec) except for a higher value of the quadrupole splitting which may be attributed to the thinness of the ion beam mixed film and to the damage imparted to the interface structure due to the ion bombardment. The hyperfine parameters of the other doublet can be favourably compared to those of hydrated non-magnetic oxides of Fe (Terrell and Spijkerman 1968; O'Grady 1980; Eldridge *et al* 1982) such as,  $\gamma$ -FeOOH (I. S. = 0.38 mm/sec, Q. S. = 0.59 mm/sec),  $\beta$ -FeOOH, (I. S. = 0.37 mm/sec, Q. S. = 0.71 mm/sec) and also  $\alpha$ -Fe<sub>2</sub>O<sub>3</sub> clusters (Kundig *et al* 1966) (I. S. = 0.31 mm/sec and Q. S. = 0.98 mm/sec).

As indicated earlier, the local atomic coordinations in the ion beam mixed alloy fluctuate within the mixed region and hence formation of two or more phases of the above type is indeed possible. Also these phases have been established to be the components of the passive films on iron surface, and as such the observed passivity, obtained in the ion beam mixed sample can be attributed to the growth of the above mentioned phases on the sample surface. The small difference between the hyperfine parameters of the passive film on the ion beam mixed surface and the above mentioned phases may be due to the presence of aluminium in the matrix. This interesting point which concerns with the internal compound states of an alloy needs further investigation. We are presently investigating the influence of ion dose, which leads to the growth of the ion beam mixed region as well as changes in its microstructural properties on the corrosive behaviour of ion bombarded Fe-Al composites. Further work employing the CEMS method to study the oxidation properties of ion beam mixed phases and the formation of amorphous oxides by ion beam mixing technique is also in progress in our laboratory.

#### 4. Conclusions

In view of the important role played by surfaces and interfaces in a variety of physical and chemical processes, there is a growing interest in both the modification of surfaces to the required specifications and characterization of surfaces at the atomic level. So far as surface modification is concerned the newer techniques such as ion implantation, ion beam mixing, electron and laser beam treatment offer many advantages and novel approaches. In the characterization of radiation-processed surface layers, in addition to the conventional techniques, the technique of CEMS also proves to be extremely useful since it can bring out valuable information concerning atomistic aspects of irradiated materials.

#### Acknowledgements

The authors gratefully acknowledge the help and cooperation of the members of the 'Submicron Physics Group' of the Department of Physics, University of Poona, in carrying out the work which has been included in the present article as the contribution of the 'Poona Group'. Three of us (SBO, SVG, SMK) are also thankful to Professors P S Damle and A S Nigavekar for their help and encouragement.

This research programme has been funded by the Department of Science and Technology, Defence Research and Development Organization, Department of Electronics, Department of Atomic Energy and Council of Scientific and Industrial Research, India. The authors gratefully acknowledge the support of these funding agencies.

#### References

- Ashworth V, Grant W A, Procter R P M and Wellington T C 1976 *Curr. Sci.* **16** 396
- Bhide V G 1973 *Mössbauer effect and its applications* (New Delhi: Tata McGraw Hill Publishing Co. Ltd.)
- Carter G and Colligon J S 1968 *Ion bombardment of solids* (England: Gresham Press)
- Crowder B L (ed.) 1973 *Ion implantation in semiconductors and other materials* (New York and London: Plenum Press)

- Dearnaley G 1981 *Nucl. Instrum. Methods* **182/183** 875
- Dorik Y S, Bhide V G, Kanetkar S M, Ghaisas S V, Chaudhari S M and Ogale S B 1984 *J. Appl. Phys.* **56** 2566
- Eldridge J, Kordes M E and Hoffman R W 1982 *J. Vac. Sci. Tech.* **20** 934
- Gibbson J F, Hess L D and Sigmon T W (eds) 1981 *Laser and electron beam solid interactions and materials processing* (New York: Elsevier; North Holland)
- Godbole V P, Bhide V G, Ghaisas S V, Kanetkar S M, Chaudhari S M and Ogale S B 1984a *Mat. Res. Soc. Symp. Proc. Thin films and interfaces-II*, (eds) J E E Baglin, I A Campbell, W K Chu (Amsterdam: Elsevier) **25** 247
- Godbole V P, Bhide V G, Ghaisas S V, Kanetkar S M, Joshee R S and Ogale S B 1984b *Mat. Res. Soc. Symp. Proc. Thin films and interfaces-II*, (eds) J E E Baglin, I A Campbell, W K Chu (Amsterdam: Elsevier Science Publishing Co. Inc.) **25** 241
- Godbole V P, Chaudhari S M, Ghaisas S V, Kanetkar S M, Ogale S B and Bhide V G 1985 *Phys. Rev.* **31**(9) 5703
- Gonser U and Ron M 1980 in *Applications of Mössbauer spectroscopy* (ed.) R L Cohen (New York: Academic Press) Vol II
- Hirvonen H and Raisanen J 1982 *J. Appl. Phys.* **53** 3314
- Hoonhout D 1981 Pulsed Laser annealing of Ion-implanted silicon Ph.D. Thesis, Fom Institute, The Netherlands
- Kanetkar S M, Dorik Y S, Chaudhari S M, Ogale S B and Bhide V G 1985 *Thin Solid Films* (submitted)
- Kundig W, Bommel H, Constabaris G and Lindquist R H 1966 *Phys. Rev.* **142** 327
- Massenet O and Daver H 1976 *Solid State Commun.* **21** 25
- Mayer J W, Erikson L and Davies J A 1970 *Ion implantation in semiconductors* (New York and London: Plenum Press)
- Nasu S, Gonser U and Preston R S 1980 *J. Phys.* **C1** 385
- Ogale S B, Godbole V P, Kanetkar S M and Bhide V G 1985b *Appl. Phys. Lett.* (submitted)
- Ogale S B, Joshee R, Godbole V P, Kanetkar S M and Bhide V G 1985a *J. Appl. Phys.* **57**(8) 2915
- O'Grady W E 1980 *J. Electrochem. Soc.* **127** 555
- Oswald R S, Ron M and Ohring M 1978 *Solid State Commun.* **26** 883
- Patankar J, Bhandarkar Y V, Kanetkar S M, Ogale S B and Bhide V G 1985 *Nucl. Instrum. Methods* **B7/8** 720
- Poate J M, Foti G and Jacobson D C (eds) 1981 *Surface modification and alloying by laser, ion and electron beams* (New York and London: Plenum Press)
- Poate J M, Tu K N, Mayer J W and Wiley A (eds) 1978 *Thin films—interdiffusion and reactions* (New York: Interscience)
- Preston R S 1972 *Metall. Trans.* **3** 1831
- Sawicka B D, Drwiega M, Sawicki J A and Stanek J 1978 *Hyperfine Interact.* **5** 147
- Sawicka B D and Sawicki J A 1977 *Phys. Lett.* **A64** 311
- Sawicka B D and Sawicki J A 1981 in *Mössbauer spectroscopy-II*, (ed.) U Gonser (Berlin, Heidelberg, New York: Springer Verlag)
- Sawicki J A and Sawicka B D 1977 *Phys. Status Solidi* **B60** K41
- Sood D K 1982 *Radiat. Eff.* **63** 141
- Terrell J H and Spijkerman J J 1968 *Appl. Phys. Lett.* **13** 11
- Tsaur B Y, Liau Z L and Mayer J W 1979 *Appl. Phys. Lett.* **A71** 270
- White C W and Peercy P S (eds) 1980 *Laser and electron-beam processing of materials* (New York: Academic Press)
- Window B 1971 *J. Phys.* **E4** 401